Interpretation of Initial Magnetization Curves in Melt spun NdFeB magnets*

Affonso Lobo Almeida[1]
Fernanda Aparecida Sampaio da Silva[2]
Daniel Rodrigues[3]
Suzilene Real Janasi[4]
José Adilson de Castro[5]
Marcos Flavio de Campos[6]

Abstract

Initial magnetization curves may reveal the coercivity mechanism. The initial magnetization curves can be calculated with the Stoner-Wohlfarth model, for single domain size particles. The tested material was a commercial Magnequench (MQPB+) powder for bonded magnet manufacture. The experimental hysteresis curves are near the average between the first and fourth quadrants of the hysteresis curve, confirming the Stoner-Wohlfarth prediction, but there is evidence of a softer phase, which maybe alpha-iron magnetostatically coupled with a $Nd_2(Fe,Co)_{14}B$ matrix.

Keywords:*Magnets;Hysteresis; Coercivity; NdFeB.*

[1] *GraduateStudent, PPGEM, EEIMVR- Universidade Federal Fluminense, Volta Redonda, RJ, Brazil.*
[2] *Dr, Researcher,,PPGEM, EEIMVR- Universidade Federal Fluminense, Volta Redonda, RJ, Brazil.*
[3] *Dr, Researcher,BRATS, Cajamar, SP, Brazil.*
[4] *Dr, Researcher,IPEN, São Paulo, SP, Brazil.*
[5] *Dr, Professor, PPGEM,,EEIMVR- Universidade Federal Fluminense, Volta Redonda, RJ, Brazil.*
[6] *Dr, Professor, PPGEM, EEIMVR- Universidade Federal Fluminense, Volta Redonda, RJ, Brazil.*
[7]

1- INTRODUCTION

Melt-spun NdFeB magnets are a subject of considerable interest, and many of the recent studies have focused on cost reduction of the alloy [1-5]. An open question in literature is the coercivity mechanism in the alloys manufactured by melt-spinning, and this can be clarified by the analysis of the initial magnetization curve.
This evaluation of the coercivity mechanism can be done with the Stoner-Wohlfarth model [6,7].

The Stoner-Wohlfarth model predicts the shape of the initial magnetization curve [6,7]. This shape is given by the average between the 1st and 4th quadrants of the hysteresis curve. The initial magnetization curve can elucidate the coercivity mechanism of SmCoCuFeZr magnets, as pointed out previously [8]. In the case of melt-spun NdFeB bonded magnets, the initial magnetization curve is near the average between first and fourth quadrants of the hysteresis [9]. The prediction was very satisfactory confirmed for Sm_2Co_{17} type magnets [10]. The objective of the present study is performing this analysis for isotropic bonded magnets made with MPQB+ powders.

1.1 - The Stoner-Wohlfarth Model

The Stoner-Wohlfarth (SW) model is described by Equation 1.

$$E = -M_S H \cos(\alpha - \phi) + K_1 \sin^2 \phi \quad (1)$$

The SW model assumes coherent rotation of single domain size particles. These particles are assumed to be non-interacting. The SW model has a large application on the modeling of magnetic materials produced by melt-spinning, which generates nanocrystalline particles [5,9]. In other words, the melt spining produces an material with grain size of the order of 100 nm or less [5,9], and this size is less than the single domain size of 300 nm for $Nd_2Fe_{14}B$ [11].

Both the isotropic [12] and anisotropic [13] Stoner-Wohlfarth model was described in previous articles. Here it will presented briefly the main equations used in modeling, i.e. Eqs (1) to (6).

From Equation 1, it is found the 1st and 2nd derivatives. By making $\frac{\partial E}{\partial \phi} = 0$ and $\frac{\partial E^2}{\partial^2 \phi} = 0$, Equation 2 and Equation 3 are found.

$$\frac{\partial E}{\partial \phi} = M_S H \sin(\alpha - \phi) - 2K_1 \sin\phi \cos\phi = 0 \quad (2)$$

$$\frac{\partial E^2}{\partial^2 \phi} = -M_S H \cos(\alpha - \phi) + 2K_1 (\sin^2\phi - \cos^2\phi) = 0 \quad (3)$$

The first derivative gives the curve m x h (Equations 4 and 5), and the second derivative gives the critical field where irreversible rotation takes place.

$$m = \cos(\alpha - \phi) \quad (4)$$

$$h = (\sin 2\phi)/(2\sin(\alpha - \phi)) \quad (5)$$

M is the reduced magnetization m=M/Ms and h is the reduced field h=H/H_A. M is magnetization and H is applied field. Ms is the magnetization of saturation, and H_A is the anisotropy field. K_1 is the first order anisotropy constant. The angle between magnetization and easy axis is ϕ, and the angle between applied field and easy axis is α. Equation 6 gives the critical angle (ϕ_c). The calculated isotropic hysteresis is presented in Figure 1.

$$\tan^3\phi_c = -\tan\alpha \quad (6)$$

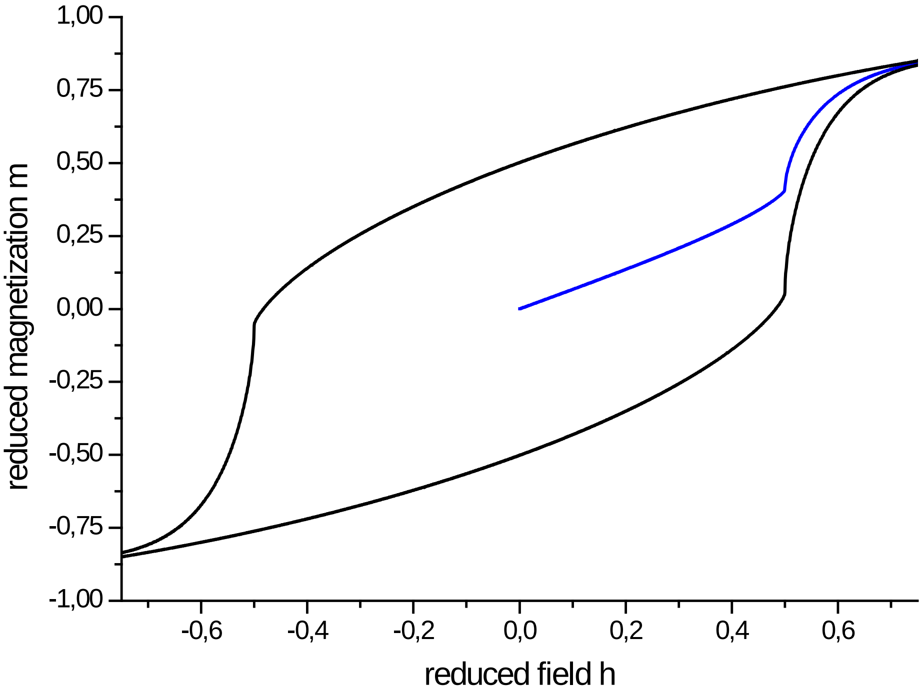

Figure 1. Initial Magnetization curve calculated with the Stoner-Wohlfarth model, for isotropic sample.

As noted by Stoner and Wohlfarth[6,7], in a thermally demagnetized sample half of the grains are magnetized in one direction and another half in another. This allows the calculation of the initial magnetization curve, as can be seen in Figure 1 (the blue curve). Here, this analysis will be applied in bonded magnets made with MPQB+ powder.

2-DEVELOPMENT

A Commercial melt spun material, from Magnequench (MQPB+), was used in this study. Cylindrical samples were pressed to densities ranging from 5.0 to 6.0 g/cm^3. Magnetic measurements were performed in a TCH-2020 (Globalmag system). Initial magnetization and hysteresis curves were determined. Three samples with 9,70 mm of diameter and 10 mm of height are analyzed in each measurement. The samples are mounted in line, for reducing the demagnetizing field. In the presented experimental hysteresis there is no correction for the demagnetizing field. The evaluated magnet is a sample with density 5.56 g/cm^3. Microstructural analysis was performed with SEM (Scanning Electron microscope) equipped with EDAX chemical analysis, Zeiss model EVO MA-10A.

The TCH2020 hysteresigraph of Globalmag was developed to measure magnetic hysteresis loops of permanent magnets under high pulsed fields. This system uses a capacitive pulse generator and air core coils to produce the magnetizing field and detect the magnetization of cylindrical samples. In the air core coils, since magnetic fields are linear to the current and to the induced voltage, both de magnetizing field and the sample magnetization can be easily estimated. The capacitive generator produces current discharges of up to 1000A with 100 ms width, generating a peak magnetizing field of 40kOe in the center of the magnetizing coil, where the sample is placed.

A search coil, wound around the sample, detects the magnetization. The search coil is composed by two concentric coils, wound in opposite directions and balanced. This topology compensates the mutual inductance between the magnetizing coil and the search coil, and allows the direct detection of the magnetization signal of the sample during the pulse. Figure 2 shows a scheme of the TCH2020 equipment.

A data acquisition module processes the electrical signals of the current and the search coil and convert them to digital data, proportional to H and M. These data are converted to Oersted and Gauss units in the data acquisition software, which traces the magnetization and the hysteresis loops. The software also allows a correction for the demagnetizing factor, since the TCH2020 operates with an open magnetic circuit.

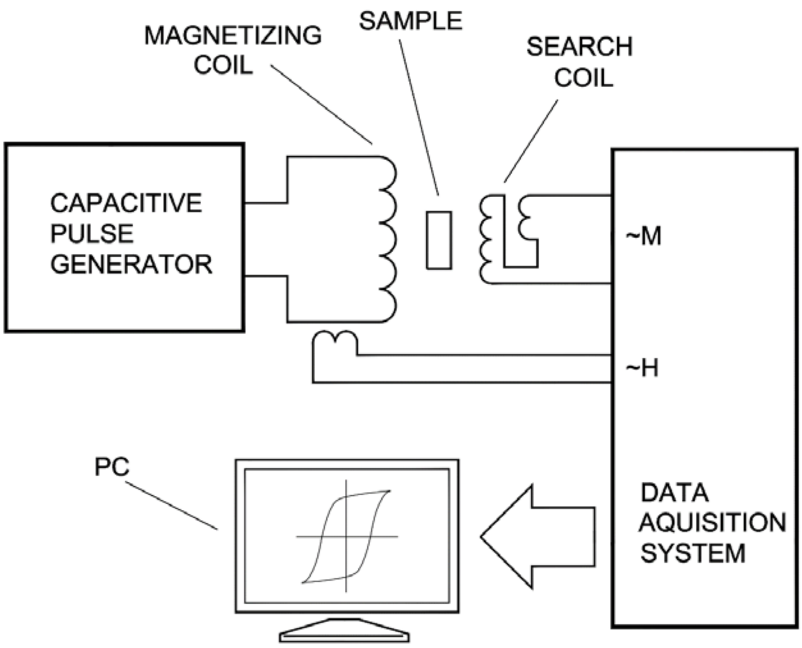

Figure 2. Scheme of the system for measurement of hysteresis and magnetic properties (Globalmag TCH2020).

2.1- Results and Discussion

The microstructural aspect of the sample is presented in Figure 3 and Figure 4. The flakes are typical of material produced by melt-spinning, as seen in Figure 4. Small addition of cobalt may improve the coercivity at temperatures a little above the room temperature. Thus cobalt is used as additive in the MQB+ powder, as seen in Figure 5. The cobalt substitutes partially iron in the $Nd_2Fe_{14}B$ structure.

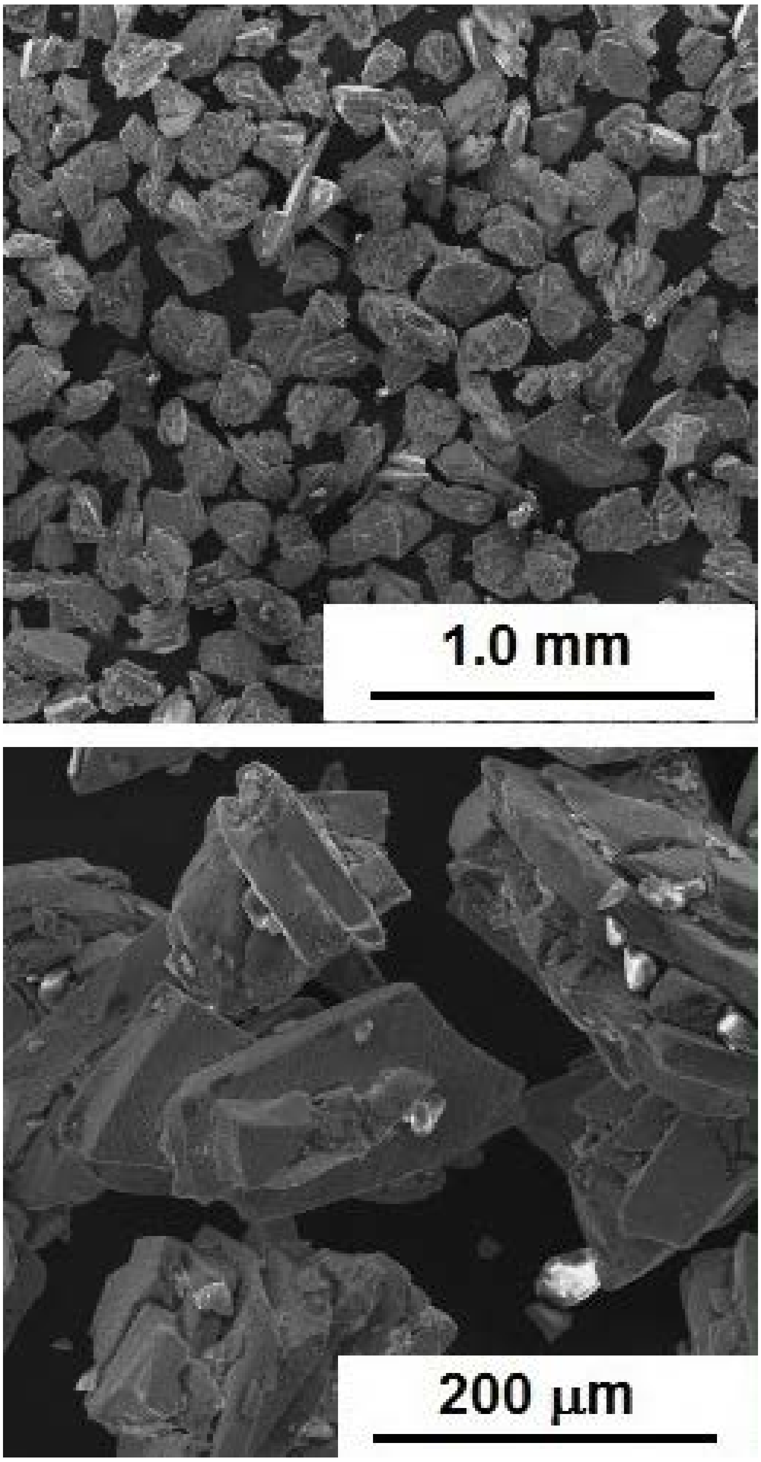

Figure 3. Ready to press MQB+ powder from MagneQuench.

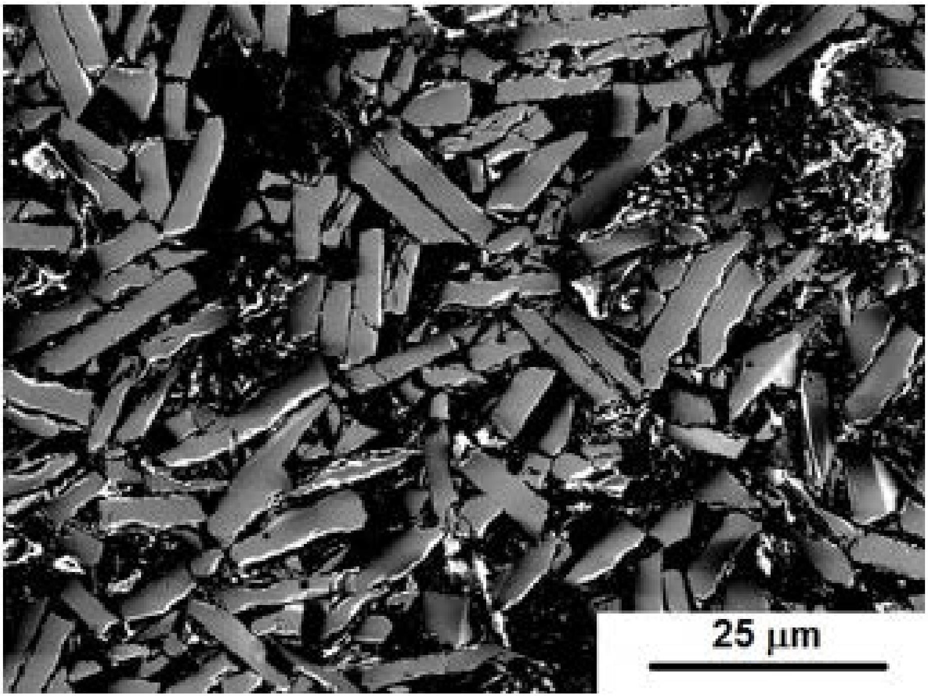

Figure 4. Aspect of bonded magnetic material after curing, showing flakes.

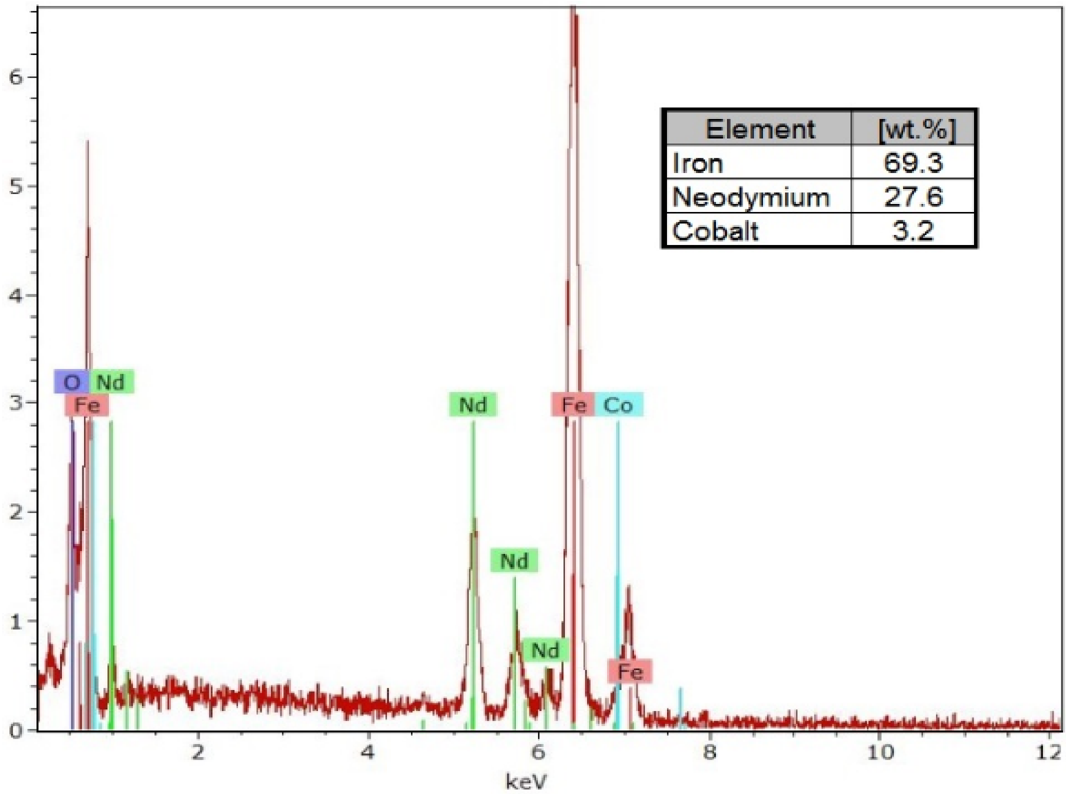

Figure 5. EDAX analysis of the powder, indicating presence of cobalt.

In the Figure 6, the complete experimental hysteresis curve is presented. In Figure 7, it is calculated the average between the 1st and 4th quadrants of the hysteresis, and it is noted that that the initial experimental curve is a little above the average. This suggests the existence of a softer magnetic phase, which reverts magnetically before the main magnetic phase, $Nd_2(FeCo)_{14}B$.

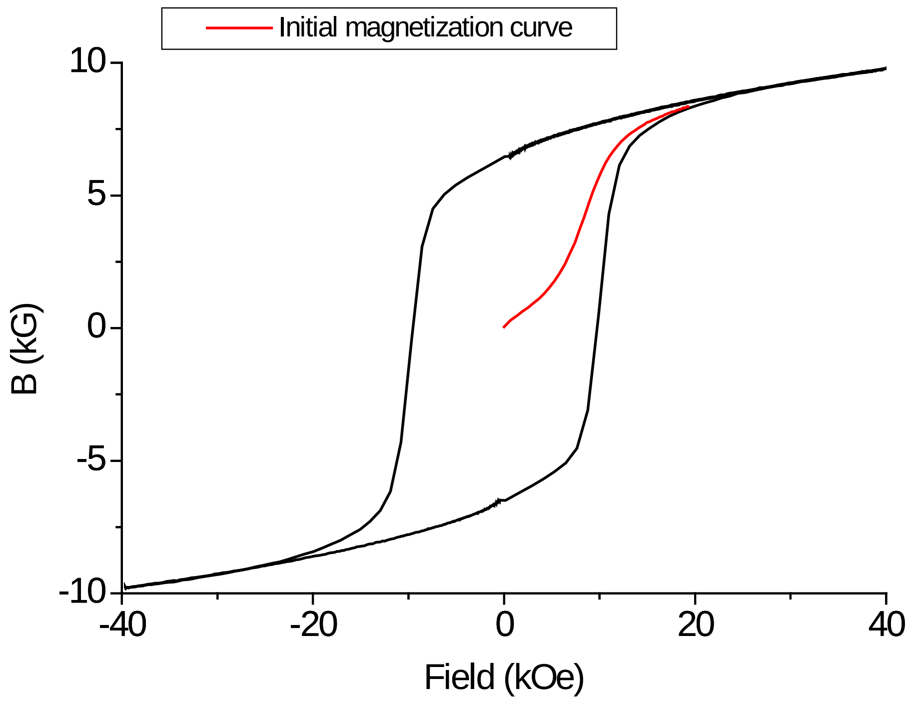

Figure 6. Experimental Hysteresis curve.

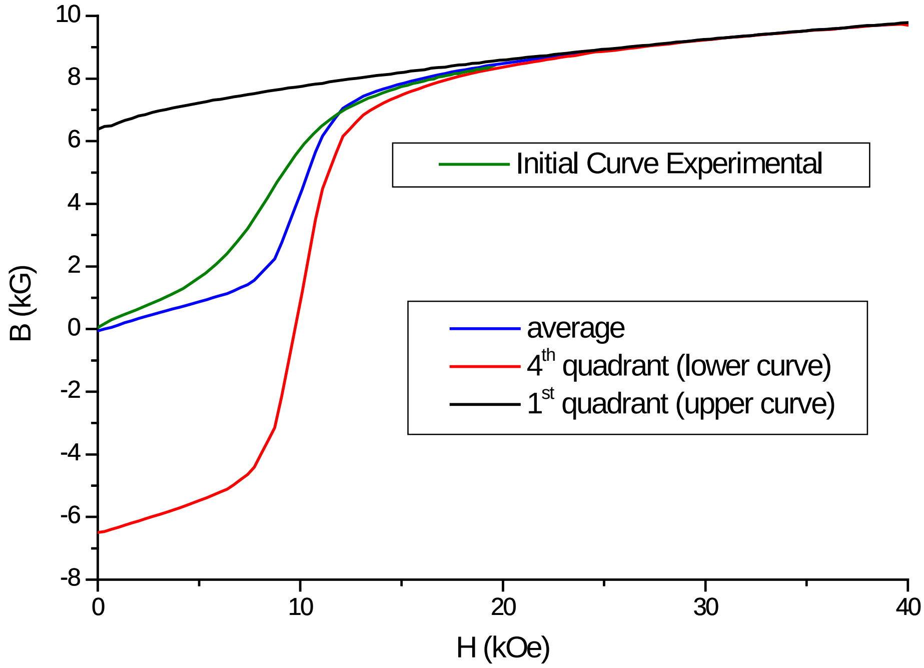

Figure 7. Analysis of the Initial Magnetization Curve

The softer phase may be a damaged oxidized layer near the surface of the sample, or may be the iron alpha phase, which is magnetostatically coupled with the matrix phase[9]. The microstructural analysis performed in a similar sample[9] indicates that both the $Nd_2(FeCo)_{14}B$ phase and the alpha iron phase are well below the single domain particle size. Thus, the SW behavior was expected for this sample.

3- CONCLUSION

The experimental hysteresis curves are near the average between the 1st and 4th quadrants of the hysteresis curve, confirming the Stoner-Wohlfarth prediction when coherent rotation is the reversal mechanism. The experimental curve indicates existence of other phase, which magnetizes more easily that the matrix phase. This soft phase maybe the alpha iron phase, which is presumably in magnetostatic coupling with the hard phase $Nd_2(FeCo)_{14}B$ or maybe also a damaged layer near the surface of the sample.

ACKNOWLEDGMENTS

Marcos Flávio de Campos and José Adilson de Castro acknowledge FAPERJ and CNPq. Affonso Henrique Lobo and Fernanda A. da Silva thanks CAPES. We thank CAPES Pro-Equipment for the Hysteresigraph.

REFERENCES

1 D N Brown, Z Wu, F He, D J Miller and J W Herchenroeder. J. Phys.: Condens. Matter 26 (2014) 064202.

2 Q. Y. Zhou, Z. Liu, S. Guo, A. R. Yan, and D. Lee. IEEE TRANSACTIONS ON MAGNETICS, 51 (2015) 2104304

3 MuNan Yang, Hang Wang, YongFeng Hu, LiuYiMei Yang, Aimee Maclennan, Bin Yang. Journal of Alloys and Compounds 710 (2017) 519-527.

4 Zhongmin Chen, Yong Keat Lim, and David Brown IEEE TRANSACTIONS ON MAGNETICS, 51, (2015) 2102104

5 R. Hirian, S. Mican, O. Isnard, L. Barbu-Tudoran, V. Pop. Journal of Alloys and Compounds 697 (2017) 19-24.

6 E.C. Stoner and E. P. Wohlfarth. *Nature*. 160 (1947), p. 650.

7 E.C. Stoner and E. P. Wohlfarth. Phil. *Trans. Royal Soc. London*. A240 (1948) 599.

8 M.F. de Campos. *Materials Science Forum*. 591–593 (2008) 8–12.

9 M. F. de Campos, S. A. Romero, F. A. S. da Silva, J. A. de Castro. J. *SupercondNov Magn*. 28 (2015) 847–850.

10 M. F. de Campos, S. A. Romero, F. J. G. Landgraf and F. P. Missell: *Journal of Physics: Conference Series*. 303 (2011) 012049.

11 J.D. Livingston. J. Appl. Phys. 57 (1985) 4137.

12 F. A. Sampaio da Silva, M. F. de Campos**.** Materials Science Forum Vols. 727-728 (2012) pp 119-123.

13 Marcos F. de Campos, Fernanda A. Sampaio da Silva, Elio A. Perigo, José A. de Castro.JournalofMagnetismandMagnetic Materials345(2013) 147–152.